Materials Chemistry and Physics 240 (2020) 121922

Contents lists available at ScienceDirect

Materials Chemistry and Physics

journal homepage: www.elsevier.com/locate/matchemphys

Room temperature ammonia gas sensor using Meta Toluic acid functionalized graphene oxide

Ravi Kumar [a], Anil Kumar [a], Rakesh Singh [a], Rajesh kashyap [a], Rajiv Kumar [b], Dinesh Kumar [a,d], Satinder K. Sharma [c], Mukesh Kumar [a,*]

[a] Electronic Science Department, Kurukshetra University, Kurukshetra, 136119, India
[b] Department of Chemistry, Kurukshetra University, Kurukshetra, 136119, India
[c] School of Computing and Electrical Engineering (SCEE), IIT Mandi, Mandi, 175005, H.P., India
[d] J.C. Bose University of Science and Technology, YMCA, Faridabad, India

HIGHLIGHTS

- Functionalized Graphene Oxide based ammonia gas sensor has been fabricated.
- Three concentration of Meta Toluic acid has been used for functionalization.
- Response has been studied in the concentration range of 100–2000 ppm of ammonia.
- The sensor shows good stability and selectivity properties.

ARTICLE INFO

Keywords:
Functionalized graphene oxide (FGO)
Graphene oxide (GO)
Gas sensor
Meta toluic acid (MTA)
Adsorption
Defects

ABSTRACT

A gas sensor has been fabricated by depositing the thin film of Functionalized Graphene Oxide (GO) using Langmuir Blodget (LB) technique on SiO_2/Si wafers. Aluminum (Al) contacts were deposited using thermal evaporation technique for measuring the resistance of fabricated thin film. Three different concentrations (15 mM, 50 mM, 75 mM) of Meta Toluic acid (MTA) have been used for functionalization of GO. X-Ray Diffraction (XRD), Fourier-transform infrared spectroscopy (FTIR) and Raman spectroscopy were used to characterize the Graphene Oxide (GO) after functionalization. Also, Scanning Electron Microscopy (SEM) was carried out for both GO and functionalized GO to study the surface morphology. Gas sensing behavior of functionalized GO has been investigated using two probe resistance measurement method for different concentration of ammonia gas. Sensor response was studied for ammonia concentration varied from 100 to 2000 ppm. Highest response obtained at 100 ppm concentration was found to be ~12.2% for sample TG_{75}. Higher concentration of MTA (up to a critical value) in GO leads to higher response of ammonia gas. This enhanced gas response has been due to the increased ester formation reaction at the surface of sensing film, which eventually leads to more interaction with NH_3 gas molecules. In addition, defects and carbon vacancy in functionalized GO also acts as the trapping sites for gas molecules being sensed. The selectivity of the sensor has been investigated in different environment and sensor was found to be very selective towards ammonia gas. For stability investigation of the fabricated sensor, the sensor response has been recorded for 45 days.

1. Introduction

The toxic gases generated from industries, vehicles and chemical waste have harmful effects on human body like skin and the respiratory system [1]. Among various gases ammonia is highly toxic and widely used in various industries. According to the Occupational Safety and Health Administration, the least amount of ammonia which is found to be irritating to the eyes, nose and throat of the most sensitive individuals is 50–100 ppm [2–6].

Direct contact of concentrated ammonia can cause serious injury like permanent eye damage. Thus, detection of these gases is very important to prevent the human hazards and surrounding environment. Many metal oxides are used for detecting combustive, oxidizing and reducing gases. Commercial metal oxide gas sensors are available for the

* Corresponding author.
E-mail address: kumarmukesh@gmail.com (M. Kumar).

https://doi.org/10.1016/j.matchemphys.2019.121922
Received 25 April 2019; Received in revised form 23 July 2019; Accepted 29 July 2019
Available online 30 July 2019

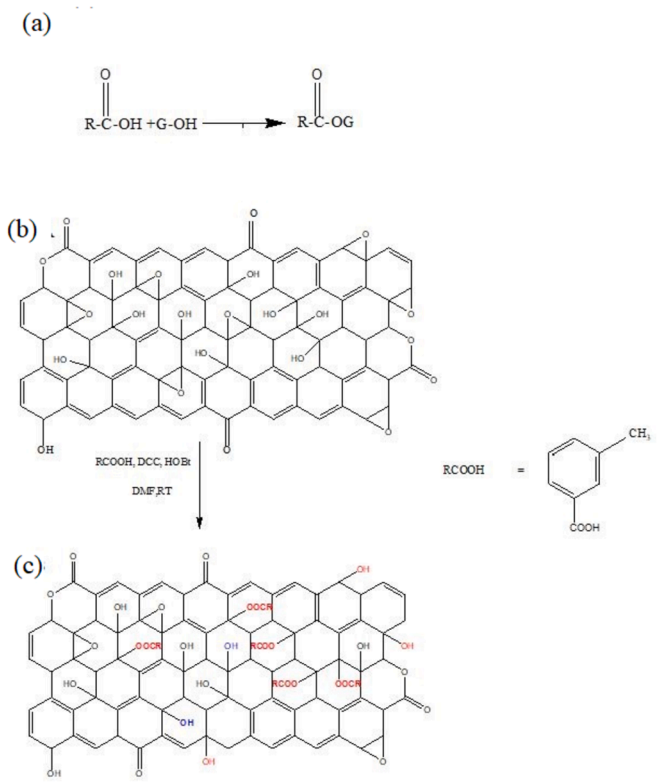

Fig. 1. (a) Mechanism representing the esterification reaction, (b) Surface Schematic of pure GO surface with different functional groups(epoxy, hydroxyl, carboxyl) present on the surface, (c) Presence of additional functional groups (ester) after functionalization of GO.

detection of ammonia gas but all theses sensors are operated at high temperature range over 200–400 °C [5] and has the drawback of short life and poor selectivity between gases [7–10]. However various other methods are available for the detection of toxic gases such as conducting polymers [11,12], carbon nanotubes [13] etc., but all these materials have some limitations. The conducting polymers have the disadvantage of poor selectivity, low response. It's not easy to achieve selective, specific response to a target species using only pure conducting polymers [14,15]. Carbon nanotube gas sensors have limitations of complex processing and high cost of fabrication [16,17]. Zhang et al. reported an ammonia sensor based on MoS_2/Co_3O_4 via a layer-by-layer self--assembly route and exhibited a significant enhancement towards NH_3 gas sensing [18]. Carbon based materials; graphene and reduced graphene oxide have been widely used in gas sensing applications because of its sp^2 hybridized 2D hexagonal honeycomb structure [19–21]. The sensing properties of Metal oxide/graphene composites were also investigated by Zhang et al. towards mixture of ammonia and formaldehyde for response sensitivity, response/recovery time at room temperature [22]. However, there is a need of developing novel gas sensing material for the development of efficient gas sensors operated at room temperature with stability and enhanced selectivity. The drawback with pristine graphene is its poor selectivity and aggregation tendency. Literature reports suggest that sensitivity response and selectivity of graphene derivates towards ammonia gas detection can be increased via functionalization or decoration with conducting polymers [23], metal oxides [24], and fluorine substitution [25] via covalent and non covalent functionalization. This is because of the fact that during functionalization we can easily control the surface chemistry which is mainly responsible for trapping of gas molecules by chemical reaction. Functionalization of graphene with high electronegative elements enhances the sensitivity towards ammonia gas [26]. katkov et al. reported a 10.2% increase in response of graphene after functionalization with fluorine for ammonia concentration at 10000 ppm [27]. However reduced graphene oxide requires additional thermal and chemical process for the reduction, thus increasing the manufacturing cost [28]. Graphene oxide(GO), decorated with various oxygen functional groups [29,30] is an ideal derivates for gas sensing application because it contains wide range of surface sites whose density can be easily controlled [31–34].

High response ammonia gas sensor (5%–23%) in the range 200–2800 ppm for chemically reduced GO was reported by Ruma Ghosh et al. [35]. Sumita et al., demonstrated the surface functionalization of GO with heteroaryl/phenyl amines by the amide formation and finds its application in gas sensing [36]. Graphene oxide gas sensor functionalized with docylamine and ethylenediamine was also reported for H_2S sensing which gave a significant response down to 50 ppm at room temperature [37]. A comparative study of gas sensing responses of fluorinated graphene oxide based gas sensor and non-treated GO was also reported by park et al. [38] which shows an approximately 7% increment in resistive response in case of fluorinated GO sensing films.

In the presented work Functionalization of GO was carried out with Meta toluic acid (MTA) using esterification reaction between GO and MTA. To the best knowledge of author this kind of work has not been carried out by any other research group. The developed sensor showed very promising and stable ammonia sensing performance. The gas sensor has the advantage of room temperature operation, has wide range detection, and no need of purging of gas and UV illumination for recovery. The ester group in the presented work acts as a linking group for the formation of hydrogen bonding with ammonia molecules. The work presents low concentration (100 ppm) detection of ammonia gas using Meta toluic acid functionalization. Long term stability and good selectivity characteristics of the sensor towards ammonia gas make this functionalization suitable for chemiresistive sensing application.

2. Experimental details

2.1. Graphene oxide preparation

GO was synthesized via chemical route using Hummer's method [39]. Natural graphite powder (5 g) was taken as precursor and mixed to Sodium Nitrate (99%), (10 g) and 230 ml of H_2SO_4 (98%). This solution was placed in ice bath with constant stirring for 45 min. After stirring, Potassium permanganate (30 g) was added into the solution in steps to maintain the temperature of solution below 20 °C (as the mixing of $KMnO_4$ with existing reactants leads to exothermic reaction). Subsequently the temperature was raised to 90 °C under constant stirring for 120 min. After that the solution was diluted with 100 ml of DI water and color of the solution changed to brown. This solution then finally treated with 30% H_2O_2 to stop the reaction and solution appearance changed to yellow color. After this step the solution was filtered using Sartorius ash free quantitative filter paper and was washed several times with DI water. For further purification of graphene oxide, thus obtained GO was sonicated for 1 h in 100 ml DI water and centrifuged for 20 min at 4000 rpm. Finally, the Synthesized GO was dried in air at room temperature for 24 h.

2.2. Functionalized GO preparation

Chemical route was used for the synthesis of Functionalized GO (FGO). Covalent coupling of Meta Toluic acid with GO was achieved using esterification reaction. Dicyclohexylcarboiimde (DCC) and hydroxybenzotriazole (HOBt) were incorporated as the reaction catalyst during synthesis of functionalized GO. These two catalysts act as a coupling agent for the formation of ester. MTA reacts with hydroxyl group present on the GO surface and results into the formation of ester group as shown in Fig. 1(a). In this figure RCOOH represents the Meta Toluic acid with carboxyl group (-COOH) and G-OH represents the graphene oxide with hydroxyl group (-OH).

20 mg of GO was dispersed in 10 ml DMF and was ultrasonicated for

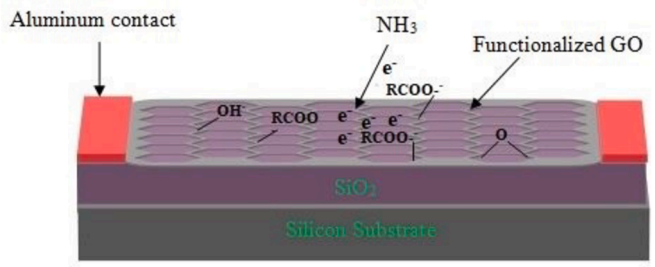

Fig. 2. The structure of the fabricated sensor.

1 h at room temperature. Separate homogeneous solution of MTA (15 mM) in DMF (20 ml) was prepared by ultrasonication at room temperature. After this, both solutions were mixed together with constant stirring at 27 °C for 30 min. Then, the temperature of the solution was raised to 70 °C under continuous stirring for 3 h. After this step, DCC and HOBt in powder form were added in the mixture and kept under continuous stirring for 24 h. Further stirring for 36 h was done at room temperature. Functionalized GO powder was collected by centrifugation process and washed with DMF and DI water many times to remove side products and to obtain pure FGO. Thus, obtained FGO powder was dried in oven at 80 °C for 12 h. Similar steps were followed by increasing the MTA concentration (50 mM & 75 mM) for synthesis of TG_{50} and TG_{75} respectively. Fig. 1(a) represents the formation of ester and the detailed Schematic diagram of coupling of Meta Toluic acid on GO surface using esterification reaction is shown in Fig. 1(b and c).

2.3. Sensor device fabrication

P-type (100) silicon wafer with resistivity of 10 Ω cm and thickness of 380 ± 10 μm was used to prepare the sensor substrate. Silicon wafer was cleaned by RCA (Radio Corporation of America) cleaning method. After cleaning of silicon wafer a thin film of SiO_2 was grown by dry oxidation process. Thickness of SiO_2 was ~110–120 nm, as measured by Laser ellipsometer. The thin film of sensing material was coated on as prepared substrate by Langmuir-Blodgett assembly (LB) technique. This technique is quite useful to form homogeneous and uniform thin film. Good homogeneous suspension of the depositing material was prepared by dispersion of 30 mg of the functionalized GO in 20 ml of DMF and ultrasonicates the solution for ~1 h. As prepared suspension was used for coating the thin film of sensing material on the substrate surface.

Deposited thin films were annealed at a temperature of 100 °C for 1 h to obtained good adhesion and better uniformity. The thickness of the film was measured by surface profiler and was found to be ~100 nm. Top Aluminum electrodes were deposited on the both sides of the substrate for electrical measurements. The aluminum contacts were deposited on the substrate by thermal vacuum coating system followed by annealing at 50 °C. Thus prepared samples were examined for the detection of Ammonia gas via two probe method. Fig. 2 represents the structure of the fabricated sensor.

2.4. Gas sensing measurement

Keithley source meter 2400 was used for the I–V measurement. The ammonia solution (25%) was injected into the chamber near the sensor using micro syringe. The sample was placed in the chamber and different concentrations of ammonia gas were introduced to the chamber manually via injection. I–V characteristics were measured at regular interval of time via two probe method by stepping the voltage in the range of 0 to + 5 V. The chamber was opened to introduce the fresh air for recovery process with N_2 purging. Ammonia gas sensing was carried out in a simple testing chamber as shown in Fig. 3.

The exposure of the sensor to ammonia gas resulted in a decrement in electrical resistance. Electrical response is defined as ratio in percentage:

$$\Delta R/R_0\ (\%) = (R_0\text{-}R) / R_0 \times 100 \quad (1)$$

Where R_0 = Baseline resistance of sensing film (in air).

R = Resistance of sensing film after exposure of NH_3 gas.

2.5. Material characterization

The PerkinElmer FTIR model Spectrum 65 system was used to study the functional groups present on surface of GO and FGO. KBr powder was used to prepare dry solid samples and powder was converted into pellets by mechanical press. After this, the pellets were scanned in the range of wave number 4000 to 500 cm^{-1}. Raman spectrum was recorded using Raman microscope (Renishaw in via), using a 514 nm wavelength laser with 2400 l/mm grafting. X-ray diffraction was used for the crystal phase characterization working with Cu Kα radiation of Wavelength 1.5406 Å in the 2θ range from 5° to 50°. For surface morphology, Scanning Electron Microscope (JSM-6510LV series) with high magnification and accelerating voltage of 500 V–30 KV was used. The surface morphology of thin film was carried out using atomic force microscopy (AFM) NTMDT Model Pro 47 Moscow, Russia. All measurements were carried out in non contact acoustic alternative current (AAC) mode. Thickness of SiO_2 was measured by Laser ellipsometer (SENTECH SE400adv). Keithley source meter 2400 was used for the I–V measurement. The thickness of the film was measured by surface profiler (AMBIOS, XP-1).

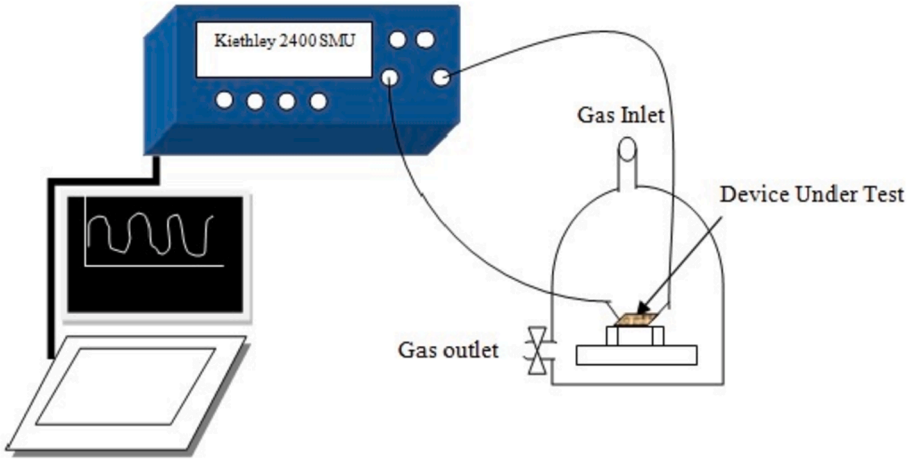

Fig. 3. Experimental set up used for the sensing of functionalized GO.

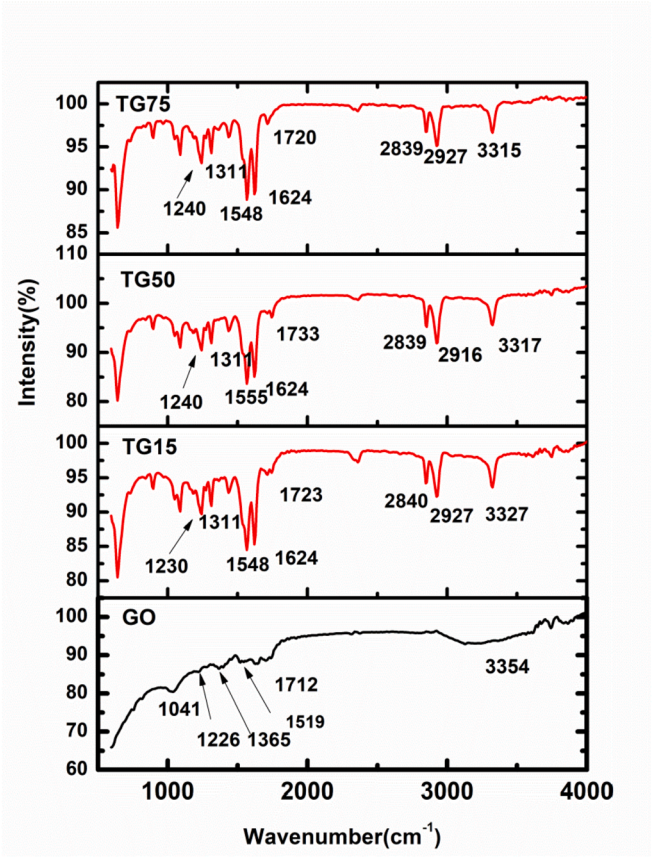

Fig. 4. FTIR spectrum of GO and Functionalized GO.

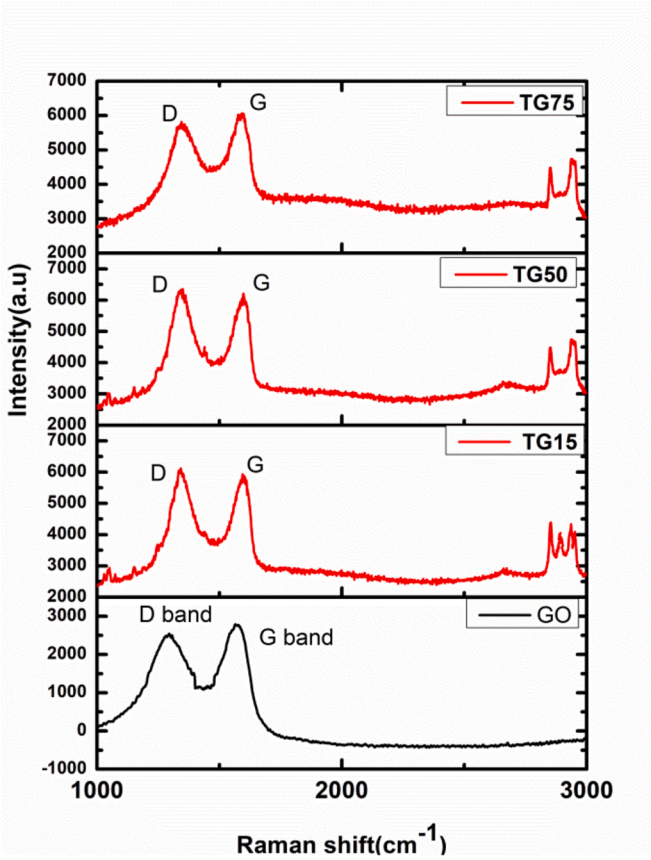

Fig. 5. Raman spectrum of GO and Functionalized GO.

3. Results and discussion

3.1. FTIR spectroscopy

The FTIR spectroscopy was used to study the functional groups present on surface of GO and FGO as shown in Fig. 4. The peaks were detected at 1365 cm^{-1} and 1041 cm^{-1} in the spectrum of GO which are assigned to the C═O stretching vibration and C═O vibrations from alkoxy groups respectively [40–42]. Broad Peaks near 3354 cm^{-1} are due to stretching vibrations of O–H bond and peaks at 1519 cm^{-1} are due to sp^2 character of C═C bond respectively [43].

The esterification of GO was verified by changes observed in the FTIR of FGO. Detection of new peaks near 1624 cm^{-1} was caused by ester formation in all FGO samples. Peaks near 2840 cm^{-1}, 2839 cm^{-1}, 2927 cm^{-1} and 2916 cm^{-1} in functionalized GO were due to the addition of aromatic ring onto the FGO surface. The O–H stretching becomes narrow in functionalized GO because of the esterification reaction between OH group of GO and COOH groups of Acid as shown in Fig. 4. New Peaks appeared near 1624 cm^{-1} was caused by esterification in Functionalized GO.

3.2. Raman spectroscopy

A Raman spectrum of the GO and functionalized GO is shown in Fig. 5. Raman spectrum of pristine graphite shows strong G peak located at 1582 cm^{-1}, weak D line at 1332 cm^{-1} and the 2D line at 2695 cm^{-1} [44]. For GO, G and D bands were observed at 1570 cm^{-1} and 1312 cm^{-1} respectively and 2D line disappeared. Almost similar results were observed in case of shapes and positions of G and D peaks for all FGO sample. As compared with graphite, significant increase in the I_d/I_g ratio was observed due to decrease in size of the in plane sp^2 domains [45,46]. The I_d/I_g ratio of GO was measured as 0.81 whereas FGO samples have I_d/I_g ratios equal to 0.95, 1.02, 1.13 for different concentration of MTA labeled as TG_{15}, TG_{50} and TG_{75} respectively. The I_d/I_g ratio of GO and functionalized GO are shown in Table 1. This increase in I_d/I_g value represents an increase in defects in the FGO structure.

Table 1
The I_d/I_g ratio value for Graphene oxide and functionalized GO obtained from XRD.

Sample	Id/Ig ratio
GO	0.81
TG_{15}	0.95
TG_{50}	1.02
TG_{75}	1.13

In FGO, the Raman spectrum of the G band gives a good representation of the sp^2 bonded carbon atom shifted near ~1601 cm^{-1},1599 cm^{-1}, 1590 cm^{-1} (for TG_{15}, TG_{50}, TG_{75}) from 1570 cm^{-1} as in case of GO. The D-band was observed at 1342 cm^{-1}, 1343 cm^{-1} and 1345 cm^{-1} (for TG_{15}, TG_{50}, TG_{75}) as compared to GO (1312 cm^{-1}). The 2D peak in the Raman spectrum of FGO was observed which strongly suggests the restoration of sp^2 carbon in FGO. The presence of 2D & 2G' (at higher wave number 2941 cm^{-1}) peaks confirms the presence of defects on the surface of FGO [47–49].

3.3. X-ray diffraction

X-ray diffraction pattern for graphite (GR), GO and functionalized GO (TG_{15}, TG_{50} and TG_{75}) is shown in Fig. 6. Diffraction peak at $2\theta = 9.9°$, is the characteristics peak of the GO. From XRD characterization it is clear that interlayer spacing('d') of GO increases to 0.88 nm as compared to GR (d = 0.33 nm), which is because of incorporation of oxide functionality to the graphite basal plane [49]. The most intense

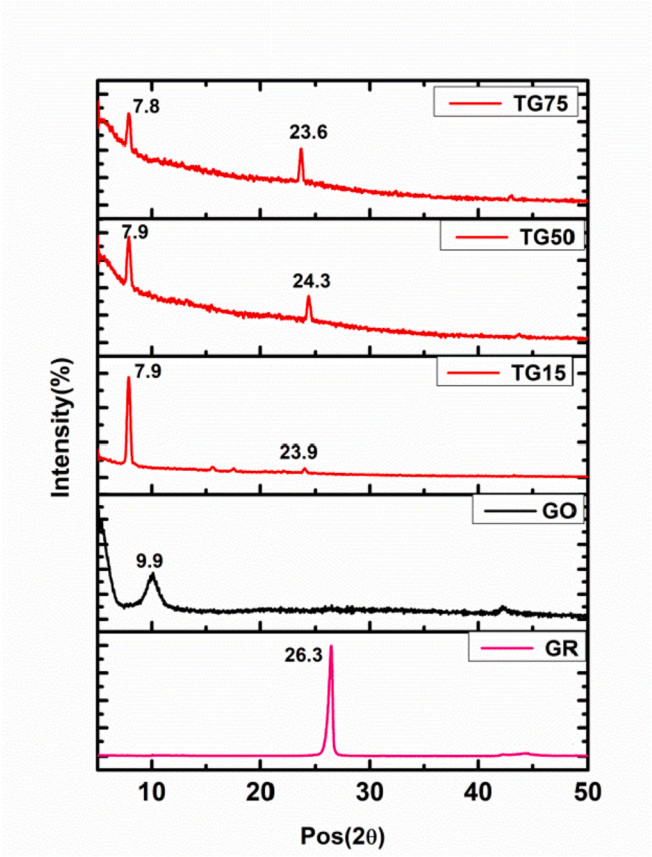

Fig. 6. X-Ray diffraction of Graphite, GO and functionalized GO.

Table 2
The peak position and'd' spacing value for Graphite, Graphene oxide and functionalized GO obtained from XRD.

Parameter	Peak (2θ)	d-Spacing(nm)	FWHM (2θ)
Graphite(GR)	26.3	0.33	0.3840
GO	9.9	0.88	1.344
TG_{15}	7.9	1.12	1.152
TG_{50}	7.9	1.12	1.152
TG_{75}	7.8	1.13	1.152

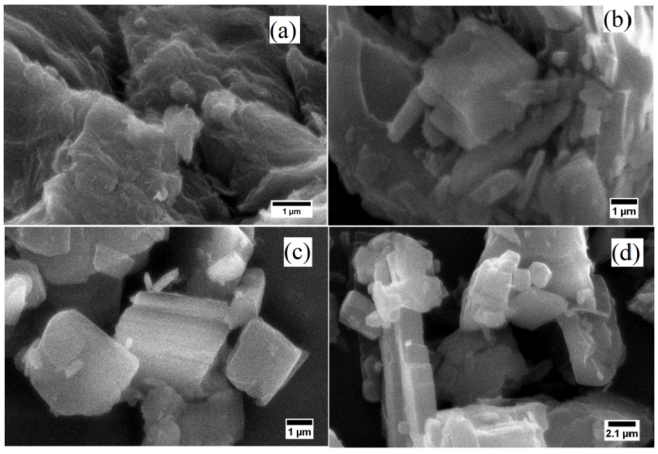

Fig. 7. (a) SEM images of GO and (b–d) Functionalized GO (TG_{15}, TG_{50}, TG_{75}) respectively.

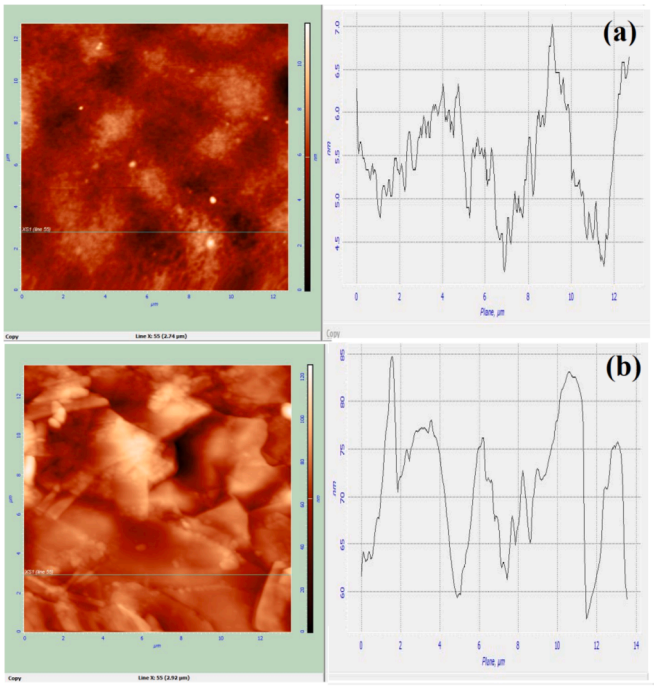

Fig. 8. AFM images and average roughness of the (a) GO and (b) Functionalized GO.

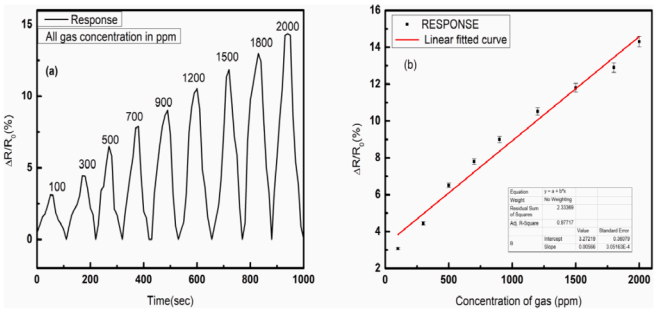

Fig. 9. (a) Response of TG_{15} with different concentration of ammonia with time (b) Response of sensing material TG_{15} with Different concentration of ammonia gas.

peak for graphite which was present at $2\theta = 26.43^{\circ}$ is not seen in the X-ray diffraction of GO sample. It is an indication of successful formation of GO by the oxidation of graphite powder. In the case of functionalized GO, the characterization peak of GO at 9.9° is shifted to 7.9° and interlayer distance further increased to ~1.13 nm as shown in Table 2 With functionalization of GO the inter layer spacing increases due to the embodiment of more functionality on the GO surface. The thickness of the film was measured by surface profiler and was found to be ~100 nm.

3.4. Surface morphology

To study the surface morphology of GO and FGO Scanning electron microscopy was carried out. Surface changes were observed using SEM images as shown in Fig. 7. SEM image shows some morphology changes in FGO in comparison to GO. In case of GO, the morphology have wrinkled surface which indicates its layered structure and functionalization of GO results in a formation of huddle structure as observed in surface morphology of FGO. Therefore some surface morphology changes takes place after functionalization. Fig. 8 (a&b) represents the AFM images of the GO and Functionalized GO. The AFM images represent some layered structure of the functionalized GO. The average

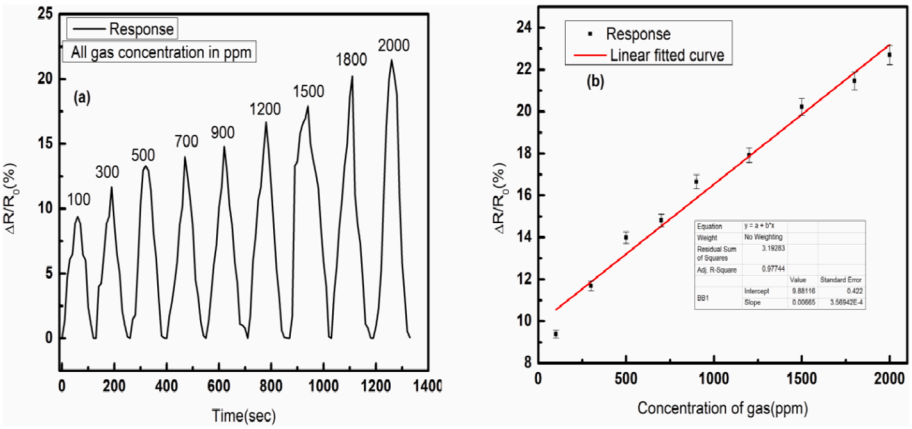

Fig. 10. (a) Response of TG_{50} with different concentration of ammonia with time (b) Response of sensing material TG_{50} with different concentration of ammonia gas.

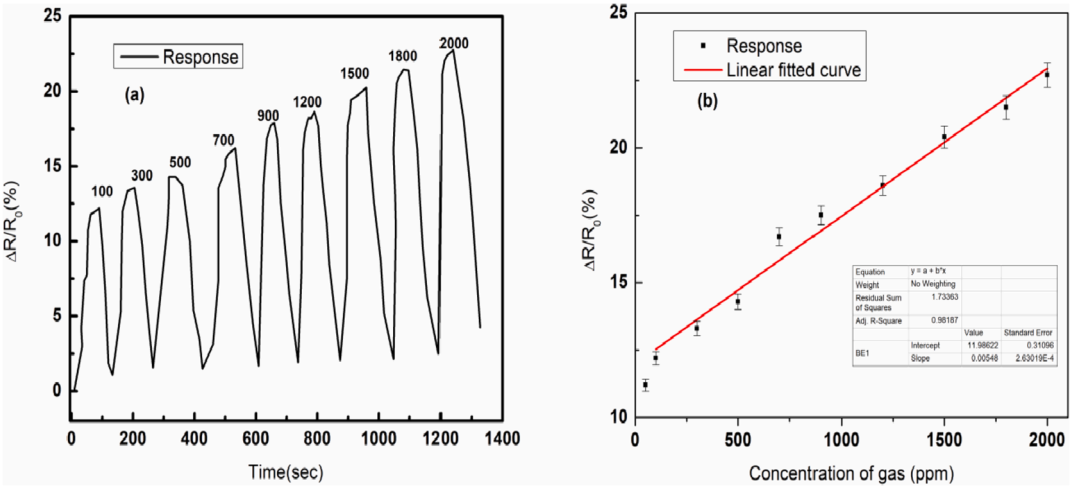

Fig. 11. (a) Response of TG_{75} with different concentration of ammonia with time (b) Response of sensing material with different concentration of ammonia gas.

Table 3
Gas sensor response for TG_{15}, TG_{50} & TG_{75} sample.

Gas Concentration (ppm)	Sensor response (%) Sample label TG_{15}	Sensor response (%) Sample label TG_{50}	Sensor response (%) Sample label TG_{75}
100	3.1	9.3	12.2
2000	14.3	22.6	22.7

Table 4
Response and recovery time for different concentration of functionalized material.

Sample	Response time	Recovery time
TG15	~55	~50
TG50	~60	~65
TG75	~60	~80

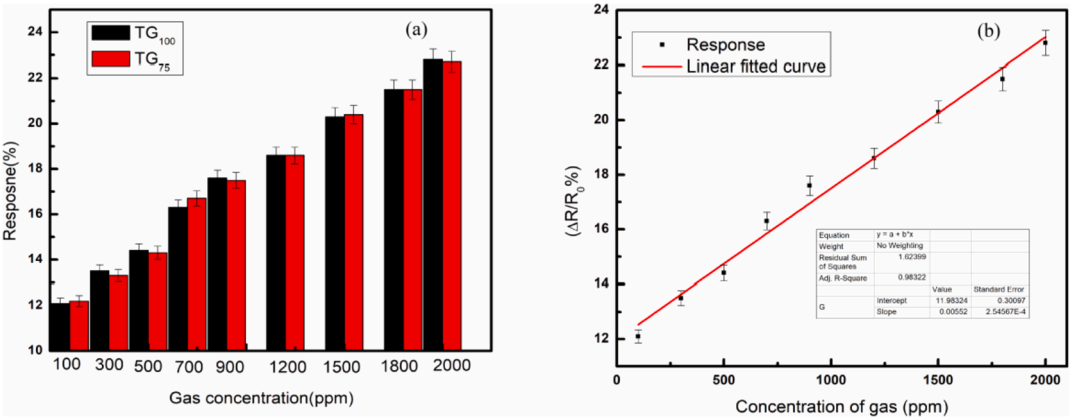

Fig. 12. (a) Comparison of response for sample TG_{75} & TG_{100} (b) Response of sensing material TG_{100} with different concentration of ammonia gas.

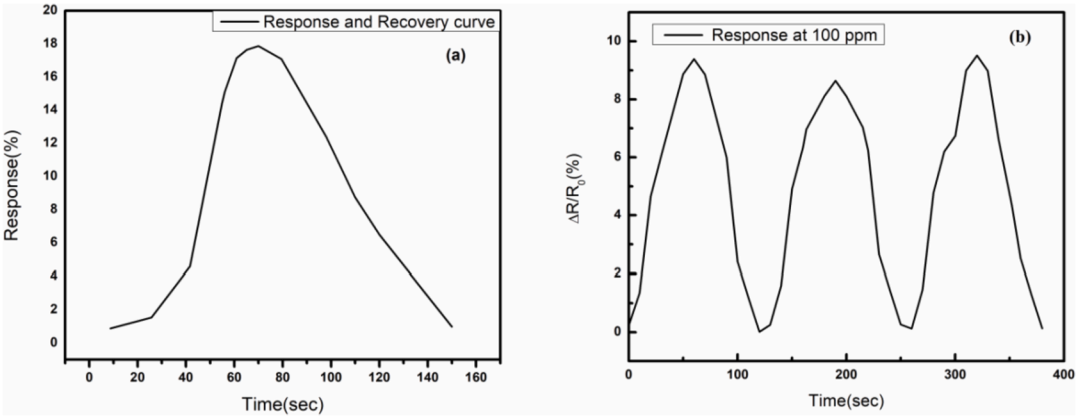

Fig. 13. (a) Response and Recovery time of the sensor (b) Represents the repeatability of the sample TG_{50} for three consecutive cycles.

Table 5
Comparative studies with previous works reported by other researchers.

Sensing material	NH_3 conc. in ppm	Response (%)	Fabrication method	Reference
SnO2/rGO	300	4.73	Hydrothermal/ self assembly	[57] (2017)
F-doped graphene	1000	10.2	Fluorinated using saturated vapors	[23] (2015)
rGO_{TA} functionalized	1310–6550	9.3–20.1	Drop cast	[56] (2014)
Meat Toluic acid functionalized GO(TG_{75})	**100**	**12.2**	**L-B technique**	**Present work**
PANI/Graphene	100	11.33	Magnetron sputtering	[58] (2013)
Pristine GO (RH 27%)	500	10	Spray coating	[59] (2017)
RGO	200	5.5	Dipping method	[36] (2013)
PANI/MWCNT	100	1.6	Drop cast	[60] (2008)
Reduced GO decorated by TiO_2 microspheres	30	3.2	Drop cast	[61] (2016)

roughness (S_a) was measured using the AFM for GO (Sa = 0.79847 nm) and functionalized GO (S_a = 9.953 nm) and it has been observed that the average roughness increases in functionalized GO which might be due to the increase in disorder on GO Surface after functionalization [50].

3.5. Gas sensing properties

Three prepared Samples of functionalized material labeled as TG_{15}, TG_{50} and TG_{75} were characterized for a range of 100 ppm–2000 ppm concentrations of ammonia gas. For concentration range (i.e. 100 ppm–2000 ppm), of ammonia gas the maximum response of the sensor was observed from 12% to 22.7% in sample TG_{75} as compared to Sample TG_{15} & TG_{50} as shown in Figs. 9–11 and Table 3.

The interaction between NH_3 and FGO would lead to the donation of negative charge carriers to FGO surface due to electron donating tendency of NH_3. Thus, the charge carrier transfer enhances the negative charge carrier density of all samples (i.e. TGO_{15}, TGO_{50} and TGO_{75}) leading to decrease in overall electrical resistance [51,52]. The sensor shows increase in response with the increase in ammonia concentration. It appears that the response varies linearly from 100 ppm to 2000 ppm as shown in Figs. 9–11. The low response of sample TG_{15} & TG_{50} at low ppm might be due to insufficient adsorption of ammonia gas molecules on the sensor surface. The low adsorption results in less chances of chemical bonding of ammonia molecules with ester groups on FGO surface.

From Table 3 it has been observed that the sample TG_{75} has the highest sensor response among all the concentrations. One reason for this fact might be due to the increased number of ester formation on functionalized GO surface. Secondly, the number of defect sites also increased at higher concentration of MTA as observed by I_d/I_g ratio in Raman Spectra. Increased number of defect sites helps in enhanced trapping of ammonia gas molecules and hence results in high sensor response. Surface defects have a key role on the sensing enhancement of the sensor and increases the effective gas adsorption on the surface which leads to the high response to gas species [51].

To investigate the effect of further increment of MTA concentration on sensor response, an experiment was performed with higher concentration i.e. 100 mM concentration of Meta Toluic acid. It has been observed that increase in the MTA concentration beyond 75 mM does not result into increment in sensor response. The reason for this might be that almost all –OH group present on GO surface have been bonded with

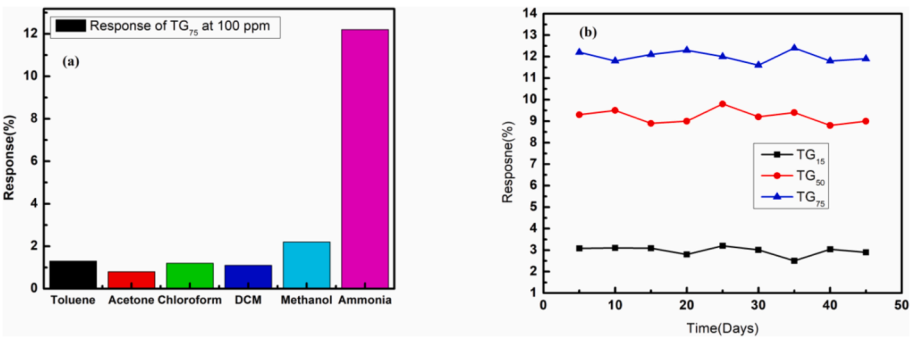

Fig. 14. (a) Selectivity investigation of sample TG75 in different environment (b) Long term stability of the sensor device.

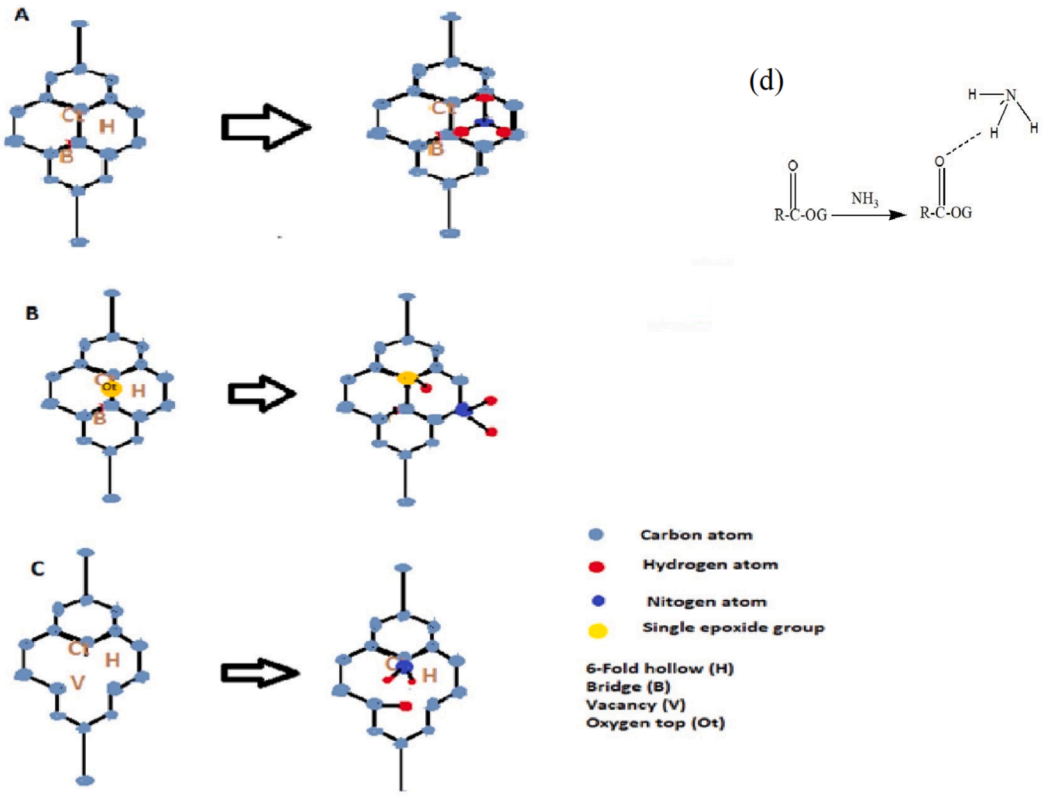

Fig. 15. Structural representation of functionalized GO and NH_3 adsorption (A) Functionalized GO before and after NH_3 adsorbed at hollow sites (B) Functionalized GO with single epoxide group (represented by yellow colored dot) and after NH_3 adsorbed resulting in NH_2 and OH group at opposite C-top sites (C) Functionalized GO with carbon vacancy and after NH_3 adsorbed at defects, dissociated into NH_2 and H bonded into nearest carbon atoms, (d) Interaction between NH_3 molecule and ester via NH···O bonding.

–COOH group to form the ester (-RCOOR') group. Thus, the availability of –OH bond on GO surface saturates for a critical MTA concentration and further increment in MTA concentration the sensor response remains almost unchanged. Fig. 12 (a) shows the comparison of the sensor response for TG_{75} & TG_{100} concentration of MTA and (b) response of sensing material TG_{100} with different concentration of ammonia gas.

The response and recovery time were calculated for all samples as shown in Table 4 and Fig. 13 (a) represents response and recovery time cycle for sample TG_{75}. The response time is defined as the time required for reaching 90% of the steady response value. The recovery time denotes the time required to recover 90% of the original base line value. The response (~55–60 s) and recovery (~50–80 s) time of the present sensor was compared with others reported work. Tran et al. [53] fabricated the RGO and silver nanowire sensor for monitoring the ammonia gas with response and recovery time of 200 s & 60 s respectively. Chemically reduced graphene oxide gas sensor with best response time ~1290 s at 2800 ppm concentration of ammonia was reported by Ruma Ghosh et al. [35].

The higher recovery time in the present study might be due to the less desorption rate of ammonia gas molecules due to the chemisorptions on the sensing surface. The sensor demonstrated good repeatability for on and off cycle of ammonia gas as shown in Fig. 13(b).

The functionalized GO exhibits good ammonia gas response at room temperature as compared in Table 5 with the previous reported work.

Selectivity measurements of the functionalized GO were studied for different environment such as Toluene, Acetone, Chloroform, Dichloromethane, Methanol and Ammonia respectively. Among all the investigated gases it has been observed that functionalized GO shows higher response towards ammonia. The response of the sensor for 100 ppm concentration of ammonia was found to be almost 6 times higher than the methanol. The response of the functionalized GO at 100 ppm concentration of Toluene, acetone, chloroform DCM, methanol and ammonia were 1.3%, 0.8%, 1.2%, 1.5%, 2.1%, 12.2% respectively. Apart from selectivity another important characteristic, stability of the fabricated sensor was also investigated. The stability of the sensor device was tested for 45 days and it has been observed that the senosr exhibits stable resposne for more than one month. The samples after each elecrical measurement were placed in vacuum desiccator during the testing period. The selectivity and long term stability analysis has shown in Fig. 14(a&b).

3.6. *Sensing mechanism*

Interaction of ammonia with Functionalized GO may have various possibilities as shown in Fig. 15(a, b, c & d) [54]. Oxygen species and carbon vacancies in the FGO encourage the surface reaction with NH_3 resulting in strong chemisorbed and physiosorbed adsorbate's. The adsorption and dissociation of ammonia on functionalized surface may be responsible for modifying the structural and electronic properties of functionalized GO and the charge transfer occurs from ammonia to functionalized GO surface by the formation of surface hydrogen bonds [55]. The possible physical adsorption and dissociation mechanism of ammonia molecule has explained below.

3.6.1. *Case A*

As indicated in Fig. 15 (a). The NH_3 molecule adsorbed either on a top bridge carbon or hollow site of the functionalized graphene oxide indicates the physical adsorption of gas molecule on sensing surface.

3.6.2. Case B. NH_3/epoxide groups present at surface of FGO

In the present case, the epoxide ring present at GO surface plays a crucial role for NH_3 gas sensing. Opening of the epoxide ring may create the oxygen and carbon sites. There are two possible ways for the opening of epoxide ring at GO surface. One is, epoxide ring present at the GO surface may break during functionalization. Another possibility for the same is during the dissociation of NH_3 molecules as while interacting with sensing film, NH_3 gas molecules may dissociate into NH_2 and H. In both above mentioned cases, the dissociated NH_2 and H molecules may get chemisorbed on available carbon and oxygen sites results in the formation of chemisorbed OH and NH_2 molecule as shown in Fig. 15 (b)

3.6.3. Case C: NH_3/Carbon vacancy

Another possible mechanism for gas sensing is where NH_3 gas molecules interacts with the carbon defects sites available at FGO surface. Dissociated NH_3 molecules may adsorbed at these sites and form the sigma bonds with carbon atoms resulting in adjacent C–NH_2 and C–H bonds as shown in Fig. 15 (c).

3.6.4. Case D: hydrogen bonding with ester groups

In this case, ammonia gas molecules may interact with oxygen atom of ester group through hydrogen bonding of the H atom of NH_3, forming $H_2NH\cdots O$ bonding configuration as shown in Fig. 15 (d) [56].

The slopes of gas responses for various MTA concentrations are almost same, except the slight increase in the slope of TG_{75} sample. It indicates that sensing mechanism is almost same for all the three samples and has not varied much with the concentration of MTA. The gas sensing response may be due to cumulative effect of carbon defects/vacancy, concentration of epoxy and ester groups present on the surface of FGO. The formation of ester group on the surface of GO was confirmed by FTIR and increase in defects sites by Raman spectroscopy. The slight increase in the slope value of TG_{75} sample may be due to higher concentration of ester groups and defect sites for higher MTA concentration while preparing a composite.

4. Conclusion

Graphene oxide has been synthesized and characterized. Fucntionalization of GO has been done using different concentration of Meta Toluic acid. A room temperature gas sensor for Ammonia gas was developed using functionalized GO as a sensing layer. Synthesized sensing material was characterized using XRD, FTIR and SEM. Electrical characterization of the gas sensor was performed and it was found that the sensor response for different concentration of ammonia (100 ppm–2000 ppm) varied from 12% to 22.7% for highest concentration of MTA (75 mM) in GO. It was recorded that Response and Recovery time (~55 s & ~80 s), for the developed gas sensor was quite good for room temperature gas sensor. The sensor device has shown a response (12.2%) towards ammonia gas for 100 ppm concentration. Repeatability of the sensor has also been tested for a fixed concentration and it demonstrated good result over three cycles of gas exposure. The selectivity and long term stability investigation has been shown which demonstrate that the functionalized GO has potential application in ammonia gas sensing.

As demonstrated in the present work, the functionalization of GO can be very easy and effective approach to enhance the sensing response, response and recovery time of a gas sensor. At the same time, this approach enables the gas sensor to work at room temperature with low power consumption.

Acknowledgements

One of the Authors Ravi Kumar is thankful to the Government of India project assisted by World Bank for providing TEQIP-II (1.2) fellowship.

References

[1] M. Evyapan, A.D.F. Dunbar, Controlling surface adsorption to enhance the selectivity of porphyrin based gas sensors, Appl. Surf. Sci. 362 (2016) 191–201.
[2] B. Timmer, W. Olthuis, A. Van Den Berg, Ammonia sensors and their applications—a review, Sens. Actuators B Chem. 107 (2) (2005) 666–677.
[3] T. Becker, S.T. Mühlberger, C.B.V. Braunmühl, G. Müller, T. Ziemann, K. V. Hechtenberg, Air pollution monitoring using tin-oxide-based microreactor systems, Sens. Actuators B Chem. 69 (1–2) (2000) 108–119.
[4] M.A. Sutton, J.W. Erisman, F. Dentener, D. Möller, Ammonia in the environment: from ancient times to the present, Environ. Pollut. 156 (3) (2008) 583–604.
[5] S. Helmers, S.F. Top, J.L. Knapp, Ammonia injuries in agriculture, J. Iowa Med. Soc. 61 (5) (1971) 271–280.
[6] J.S. Mulder, H.O. Van Der Zalm, Fatal case of ammonia poisoning, Tijdschr. Soc. Geneeskd. 45 (1967) 458–460.
[7] A. Ponzoni, C. Baratto, N. Cattabiani, M. Falasconi, V. Galstyan, E. Nunez-Carmona, F. Rigoni, V. Sberveglieri, G. Zambotti, D. Zappa, Metal oxide gas sensors, a survey of selectivity issues addressed at the SENSOR Lab, Brescia (Italy), Sensors 17 (4) (2017) 714.
[8] X.J. Huang, Y.K. Choi, Chemical sensors based on nanostructured materials, Sens. Actuators B Chem. 122 (2) (2007) 659–671.
[9] D. Zhang, Q. Li, P. Li, M. Pang, Y. Luo, Fabrication of Pd-decorated MoSe 2 nanoflowers and density functional theory simulation toward ammonia sensing, IEEE Electron. Device Lett. 40 (4) (2019) 616–619.
[10] D.R. Miller, S.A. Akbar, P.A. Morris, Nanoscale metal oxide-based heterojunctions for gas sensing: a review, Sens. Actuators B Chem. 204 (2014 Dec 1) 250–272.
[11] R. Garg, V. Kumar, D. Kumar, S.K. Chakarvarti, Polypyrrole microwires as toxic gas sensors for ammonia and hydrogen sulphide, J. Sensors Instrum. 3 (1) (2015) 1–13.
[12] D. Zhang, Z. Wu, P. Li, X. Zong, G. Dong, Y. Zhang, Facile fabrication of polyaniline/multi-walled carbon nanotubes/molybdenum disulfide ternary nanocomposite and its high-performance ammonia-sensing at room temperature, Sens. Actuators B Chem. 258 (2018 Apr 1) 895–905.
[13] M. Asad, M.H. Sheikhi, M. Pourfath, M. Moradi, High sensitive and selective flexible H2S gas sensors based on Cu nanoparticle decorated SWCNTs, Sens. Actuators B Chem. 210 (2015) 1–8.
[14] S. Park, C. Park, H. Yoon, Chemo-electrical gas sensors based on conducting polymer hybrids, Polymers 9 (5) (2017 May) 155.
[15] D. Zhang, Z. Wu, X. Zong, Y. Zhang, Fabrication of polypyrrole/Zn2SnO4 nanofilm for ultra-highly sensitive ammonia sensing application, Sens. Actuators B Chem. 274 (2018 Nov 20) 575–586.
[16] S. Cui, H. Pu, G. Lu, Z. Wen, E.C. Mattson, C. Hirschmugl, M. Gajdardziska-Josifovska, M. Weinert, J. Chen, Fast and selective room-temperature ammonia sensors using silver nanocrystal-functionalized carbon nanotubes, ACS Appl. Mater. Interfaces 4 (9) (2012 Aug 20) 4898–4904.
[17] L. Camilli, M. Passacantando, Advances on sensors based on carbon nanotubes, Chemosensors 6 (4) (2018 Dec) 62.
[18] D. Zhang, C. Jiang, P. Li, Y. Sun, Layer-by-layer self-assembly of Co3O4 nanorod-decorated MoS2 nanosheet-based nanocomposite toward high-performance ammonia detection, ACS Appl. Mater. Interfaces 9 (2017) 6462–6471.
[19] A. Pourjavadi, Z.M. Tehrani, S. Jokar, Functionalized mesoporous silica-coated magnetic graphene oxide by polyglycerol-g-polycaprolactone with pH-responsive behavior: designed for targeted and controlled doxorubicin delivery, J. Ind. Eng. Chem. 28 (2015) 45–53.
[20] W. Yuan, A. Liu, L. Huang, C. Li, G. Shi, High-performance NO2 sensors based on chemically modified graphene, Adv. Mater. 25 (5) (2013) 766–771.
[21] M. Gautam, A.H. Jayatissa, Graphene based field effect transistor for the detection of ammonia, J. Appl. Phys. 112 (6) (2012), 064304.
[22] D. Zhang, J. Liu, C. Jiang, A. Liu, B. Xia, Quantitative detection of formaldehyde and ammonia gas via metal oxide-modified graphene-based sensor array combining with neural network model, Sens. Actuators B Chem. 240 (2017 Mar 1) 55–65.
[23] H. Bai, K. Sheng, P. Zhang, C. Li, G. Shi, Graphene oxide/conducting polymer composite hydrogels, J. Mater. Chem. 21 (46) (2011) 18653–18658.
[24] D. Zhang, Z. Wu, P. Li, X. Zong, G. Dong, Y. Zhang, Facile fabrication of polyaniline/multi-walled carbon nanotubes/molybdenum disulfide ternary nanocomposite and its high-performance ammonia-sensing at room temperature, Sens. Actuators B Chem. 258 (2018) 895–905.
[25] W. Kang, S. Li, Preparation of fluorinated graphene to study its gas sensitivity, RSC Adv. 8 (41) (2018) 23459–23467.
[26] S. Prezioso, F. Perrozzi, L. Giancaterini, C. Cantalini, E. Treossi, V. Palermo, M. Nardone, S. Santucci, L. Ottaviano, Graphene oxide as a practical solution to high sensitivity gas sensing, J. Phys. Chem. C 117 (20) (2013) 10683–10690.
[27] M.V. Katkov, V.I. Sysoev, A.V. Gusel'Nikov, I.P. Asanov, L.G. Bulusheva, A. V. Okotrub, A backside fluorine-functionalized graphene layer for ammonia detection, Phys. Chem. Chem. Phys. 17 (1) (2015) 444–450.
[28] D. Yang, A. Velamakanni, G. Bozoklu, S. Park, M. Stoller, R.D. Piner, S. Stankovich, I. Jung, D.A. Field, C.A. Ventrice Jr., R.S. Ruoff, Chemical analysis of graphene oxide films after heat and chemical treatments by X-ray photoelectron and Micro-Raman spectroscopy, Carbon 47 (1) (2009) 145–152.
[29] S. Choi, D.K. Hwang, H.S. Lee, Thermal properties in strong hydrogen bonding systems composed of poly (vinyl alcohol), polyethyleneimine, and graphene oxide, Carbon Lett. 15 (4) (2014) 282–289.
[30] V. Georgakilas, M. Otyepka, A.B. Bourlinos, V. Chandra, N. Kim, K.C. Kemp, P. Hobza, R. Zboril, K.S. Kim, Functionalization of graphene: covalent and non-covalent approaches, derivatives and applications, Chem. Rev. 112 (11) (2012) 6156–6214.

[31] S. Wu, Z. Yin, Q. He, X. Huang, X. Zhou, H. Zhang, Electrochemical deposition of semiconductor oxides on reduced graphene oxide-based flexible, transparent, and conductive electrodes, J. Phys. Chem. C 114 (27) (2010) 11816–11821.
[32] H.A. Becerril, J. Mao, Z. Liu, R.M. Stoltenberg, Z. Bao, Y. Chen, Evaluation of solution-processed reduced graphene oxide films as transparent conductors, ACS Nano 2 (2008) 463–470.
[33] D. Zhang, J. Tong, B. Xia, Humidity-sensing properties of chemically reduced graphene oxide/polymer nanocomposite film sensor based on layer-by-layer nano self-assembly, Sens. Actuators B Chem. 197 (2014 Jul 5) 66–72.
[34] D. Zhang, H. Chang, P. Li, R. Liu, Q. Xue, Fabrication and characterization of an ultrasensitive humidity sensor based on metal oxide/graphene hybrid nanocomposite, Sens. Actuators B Chem. 225 (2016) 233–240.
[35] R. Ghosh, A. Midya, S. Santra, S.K. Ray, P.K. Guha, Chemically reduced graphene oxide for ammonia detection at room temperature, ACS Appl. Mater. Interfaces 5 (15) (2013) 7599–7603.
[36] S. Rani, M. Kumar, R. Garg, S. Sharma, D. Kumar, Amide functionalized graphene oxide thin films for hydrogen sulfide gas sensing applications, IEEE Sens. J. 16 (9) (2016) 2928–2934.
[37] M.M. Alaie, M. Jahangiri, A.M. Rashidi, A.H. Asl, N. Izadi, A novel selective H2S sensor using dodecylamine and ethylenediamine functionalized graphene oxide, J. Ind. Eng. Chem. 29 (2015) 97–103.
[38] M.S. Park, K.H. Kim, M.J. Kim, Y.S. Lee, NH3 gas sensing properties of a gas sensor based on fluorinated graphene oxide, Colloid. Surf. Physicochem. Eng. Asp. 490 (2016) 104–109.
[39] W.S. Hummers Jr., R.E. Offeman, Preparation of graphitic oxide, J. Am. Chem. Soc. 80 (6) (1958), 1339-1339.
[40] L. Fu, W. Cai, A. Wang, Y. Zheng, Photocatalytic hydrogenation of nitrobenzene to aniline over tungsten oxide-silver nanowires, Mater. Lett. 142 (2015) 201–203.
[41] J. Zhang, H. Yang, G. Shen, P. Cheng, J. Zhang, S. Guo, Reduction of graphene oxide via L-ascorbic acid, Chem. Commun. 46 (7) (2010) 1112–1114.
[42] M. Ahmad, E. Ahmed, Z.L. Hong, J.F. Xu, N.R. Khalid, A. Elhissi, W. Ahmed, A facile one-step approach to synthesizing ZnO/graphene composites for enhanced degradation of methylene blue under visible light, Appl. Surf. Sci. 274 (2013) 273–281.
[43] P. Karthika, N. Rajalakshmi, K.S. Dhathathreyan, Functionalized exfoliated graphene oxide as supercapacitor electrodes, Soft Nanosci. Lett. 2 (04) (2012) 59.
[44] S. Stankovich, D.A. Dikin, R.D. Piner, K.A. Kohlhaas, A. Kleinhammes, Y. Jia, Y. Wu, S.T. Nguyen, R.S. Ruoff, Synthesis of graphene-based nanosheets via chemical reduction of exfoliated graphite oxide, Carbon 45 (7) (2007) 1558–1565.
[45] A. Jorio, Raman spectroscopy in graphene-based systems: prototypes for nanoscience and nanometrology, ISRN Nanotechnol. 2012 (2012) 1–16.
[46] K.N. Kudin, B. Ozbas, H.C. Schniepp, R.K. Prud'Homme, I.A. Aksay, R. Car, Raman spectra of graphite oxide and functionalized graphene sheets, Nano Lett. 8 (1) (2008) 36–41.
[47] S. Peng, C. Liu, X. Fan, Surface modification of graphene oxide by carboxyl-group: preparation, characterization, and application for proteins immobilization, Integr. Ferroelectr. 163 (1) (2015) 42–53.
[48] M.A. Pimenta, G. Dresselhaus, M.S. Dresselhaus, L.G. Cancado, A. Jorio, R. Saito, Studying disorder in graphite-based systems by Raman spectroscopy, Phys. Chem. Chem. Phys. 9 (11) (2007) 1276–1290.
[49] H.J. Salavagione, G. Martínez, Importance of covalent linkages in the preparation of effective reduced graphene oxide– poly (vinyl chloride) nanocomposites, Macromolecules 44 (8) (2011) 2685–2692.
[50] E. Peng, N. Todorova, I. Yarovsky, Effects of size and functionalization on the structure and properties of graphene oxide nanoflakes: an in silico investigation, ACS Omega 3 (9) (2018) 11497–11503.
[51] B. Kumar, K. Min, M. Bashirzadeh, A.B. Farimani, M.H. Bae, D. Estrada, Y.D. Kim, P. Yasaei, Y.D. Park, E. Pop, N.R. Aluru, The role of external defects in chemical sensing of graphene field-effect transistors, Nano Lett. 13 (5) (2013) 1962–1968.
[52] G. Lu, L.E. Ocola, J. Chen, Gas detection using low-temperature reduced graphene oxide sheets, Appl. Phys. Lett. 94 (8) (2009), 083111.
[53] Q.T. Tran, T.M.H. Huynh, D.T. Tong, N.D. Nguyen, Synthesis and application of graphene–silver nanowires composite for ammonia gas sensing, Adv. Nat. Sci. Nanosci. Nanotechnol. 4 (4) (2013), 045012.
[54] E.C. Mattson, K. Pande, M. Unger, S. Cui, G. Lu, M. Gajdardziska-Josifovska, M. Weinert, J. Chen, C.J. Hirschmugl, Exploring adsorption and reactivity of NH3 on reduced graphene oxide, J. Phys. Chem. C 117 (20) (2013) 10698–10707.
[55] S. Tang, Z. Cao, Adsorption and dissociation of ammonia on graphene oxides: a first-principles study, J. Phys. Chem. C 116 (15) (2012) 8778–8791.
[56] S. Yoo, X. Li, Y. Wu, W. Liu, X. Wang, W. Yi, Ammonia gas detection by tannic acid functionalized and reduced graphene oxide at room temperature, J. Nanomater. 2014 (2014) 1–6.
[57] D. Zhang, J. Liu, C. Jiang, A. Liu, B. Xia, Quantitative detection of formaldehyde and ammonia gas via metal oxide-modified graphene-based sensor array combining with neural network model, Sens. Actuators B Chem. 240 (2017) 55–65.
[58] Z. Wu, X. Chen, S. Zhu, Z. Zhou, Y. Yao, W. Quan, B. Liu, Enhanced sensitivity of ammonia sensor using graphene/polyaniline nanocomposite, Sens. Actuators B Chem. 178 (2013) 485–493.
[59] A. Bannov, J. Prášek, O. Jašek, L. Zajíčková, Investigation of pristine graphite oxide as room-temperature chemiresistive ammonia gas sensing material, Sensors 17 (2) (2017) 320.
[60] T.J. Kim, S.D. Kim, N.K. Min, J.J. Pak, C.J. Lee, S.W. Kim, October. NH 3 sensitive chemiresistor sensors using plasma functionalized multiwall carbon nanotubes/ conducting polymer composites, in: SENSORS, 2008 IEEE, IEEE, 2008, pp. 208–211.
[61] X. Li, Y. Zhao, X. Wang, J. Wang, A.M. Gaskov, S.A. Akbar, Reduced graphene oxide (rGO) decorated TiO2 microspheres for selective room-temperature gas sensors, Sens. Actuators B Chem. 230 (2016) 330–336.